Applied Surface Science 406 (2017) 301–306

Contents lists available at ScienceDirect

Applied Surface Science

journal homepage: www.elsevier.com/locate/apsusc

Full length article

Theoretical insight into an empirical rule about organic corrosion inhibitors containing nitrogen, oxygen, and sulfur atoms

Lei Guo[a,*], Ime Bassey Obot[b], Xingwen Zheng[c], Xun Shen[a], Yujie Qiang[c], Savaş Kaya[d], Cemal Kaya[d]

[a] School of Material and Chemical Engieering, Tongren University, Tongren 554300, China
[b] Center of Research Excellence in Corrosion, King Fahd University of Petroleum and Minerals, Dhahran 31261, Saudi Arabia
[c] Material Corrosion and Protection Key Laboratory of Sichuan province, Zigong 643000, China
[d] Department of Chemistry, Faculty of Science, Cumhuriyet University, Sivas 58140, Turkey

ARTICLE INFO

Article history:
Received 19 August 2016
Received in revised form 14 February 2017
Accepted 16 February 2017
Available online 20 February 2017

Keywords:
Density functional theory
Corrosion inhibitor
Steel
Adsorption

ABSTRACT

Steel is an important material in industry. Adding heterocyclic organic compounds have proved to be very efficient for steel protection. There exists an empirical rule that the general trend in the inhibition efficiencies of molecules containing heteroatoms is such that O < N < S. However, an atomic-level insight into the inhibition mechanism is still lacked. Thus, in this work, density functional theory calculations was used to investigate the adsorption of three typical heterocyclic molecules, *i.e.*, pyrrole, furan, and thiophene, on Fe(110) surface. The approach is illustrated by carrying out geometric optimization of inhibitors on the stable and most exposed plane of α-Fe. Some salient features such as charge density difference, changes of work function, density of states were detailedly described. The present study is helpful to understand the afore-mentioned experiment rule.

1. Introduction

Because of the excellent mechanical properties and cheapness, steel is widely utilized as the constructional material in most industrial fields. However, they generally face the corrosion problems, that is the degradation of steel by a chemical or electrochemical reaction with its environment. This usually causes enormous economic losses and many potential security problems, and anti-corrosion technology has received increasing interest among researchers [1–3]. The application and addition of organic corrosion inhibitors has become one of the most effective and economic methods. It can protect metal from being corroded through low consumption [4,5]. Most reports suggest that the organic inhibitors function by the adsorption effect with the metal surface [6–9], and the adsorption of inhibitors takes place through heteroatoms (nitrogen, oxygen, sulphur, etc.), as well as through double/triple bounds or aromatic rings. The inhibition efficiency is reported to follow the sequence O < N < S. This is not understandable, due to oxygen atom has a larger electronegativity (χ) value than nitrogen and sulphur (*i.e.*, $\chi_O = 3.44$, $\chi_N = 3.04$, $\chi_S = 2.58$) atoms. Thus, as Fig. 1 shows, the outer electrons are firmly held around the oxygen atom. However, as for nitrogen and sulphur, their donor ability enhanced in turn. The correctness of this empirical rule has been experimentally verified many times by some researchers [10–12].

For most of the past few decades, a considerable amount of experimental methods have been adopted to evaluate the inhibition performance and mechanism of organic corrosion inhibitors, such as weight-loss method, electrochemical methods, and scanning electron microscopy techniques. More detailed names for these methods are displayed in Fig. 2. Current experimental approaches to assess and select inhibitors are expensive and labor-intensive, which represents an impediment to progress. Although teams of researchers have pointed out that the organic molecules inhibit the corrosion process by adsorption on the metal surface, the adsorption configurations of the inhibitors/metal systems remain unclear, and it is also very difficult to obtain these with experimental methods.

Generally, there are mainly two kinds of attractions leading to absorption of inhibitor molecules onto metal surface, physical adsorption and chemical adsorption. The latter plays a major role in the interaction processes. Actually, most researchers prefer studying the absorption using molecular dynamics simulation method based on COMPASS force field, which possesses cheap, simple, and

* Corresponding author.
E-mail address: cqglei@163.com (L. Guo).

http://dx.doi.org/10.1016/j.apsusc.2017.02.134
0169-4332/

Table 1
Calculated surface energy values and several morphology parameters for Fe crystal.

hkl	Multiplicity	d_{hkl}	Surface area (Å^2)	Total facet area ($\times 10^8$ Å^2)	%Total facet area	E_{surf} (J/m^2)
(110)	12	2.026	5.809	8.65	63.98	2.887[a] 2.288[b]
(100)	6	1.433	8.216	3.32	24.54	3.082[a] 2.301[b]
(111)	8	0.827	14.230	1.55	11.47	3.114[a] 2.586[b]

[a] The values were calculated by CASTEP module in this work.
[b] Ref. [25].

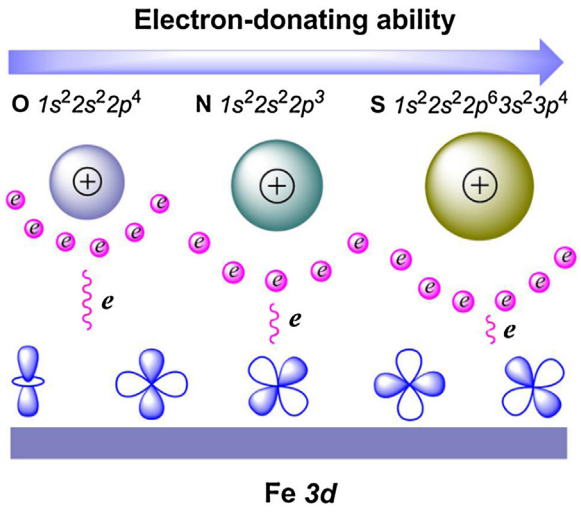

Fig. 1. Schematic diagram of the electron donating ability comparison among the O, N, and S atoms.

fast features. Unfortunately, we can only perform qualitative analysis by this way, and it is very embarrassing for force field to describe the electron transfer processes.

In recent years, density functional theory (DFT), which is a reliable and inexpensive method, has been used to examine the molecular activity and the interaction of adsorbates with the metal surface [13–16]. The advantage here is that this approach provides relatively intuitive informational content about the contacts between organic corrosion inhibitors and metal surfaces. It is effective to reveal the impact of minor modifications in the structures of organic active compounds on their inhibition efficiency, and is helpful to develop novel corrosion inhibitor molecules in an efficient and cost-effective manner for use in a number of corrosion systems for domestic and industrial applications.

To better understand the inhibiton mechanism, we performed DFT calculations on the adsorption behavior of three typical heterocyclic molecules, *i.e.*, pyrrole, furan, and thiophene, on clean iron surfaces. The most stable adsorption configurations, charge density difference, changes of work function, density of states have been theoretically reported.

2. Computational details

Firstly, to have a full knowledge of the iron surface, we decided to predict its crystal structures using equilibrium morphology method [17]. The "Morphology" prediction sequence generates and outputs a list of possible growth planes that satisfy the Donnay-Harker rules for the current symmetry. It combines the CASTEP modules, both available from the Materials Studio (MS, version 7.0) program package of Accelrys Inc., were adopted to elaborate the reason why we chose Fe(110) surface as research subject.

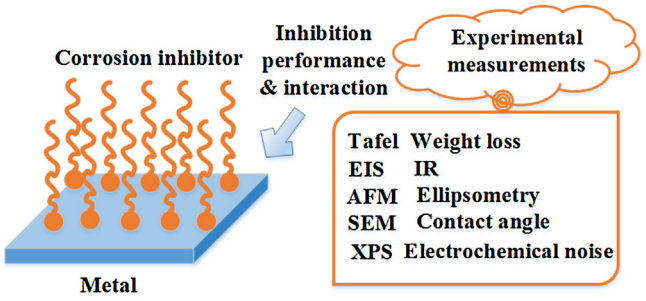

Fig. 2. Some typical experimental methods used in studying the inhibitive efficiency & mechanism.

The interactions between the inhibitors molecules and Fe(110) surface was performed in a simulation box with periodic boundary conditions employing the DMol^3 code [18] (also embedded in MS). In the DMol^3 program, the plane wave functions were expanded in terms of accurate numerical basis sets, which were constructed specifically for use in DFT calculations.

The Fe(110) surface was modelled by periodic slab models consisting of four atomic layers. Although the adopted thickness is slightly inferior compared to some samll C/H–Fe(110) adsorption systems [19,20], it is sufficiently thick to serve as adsorption substrate as confirmed by previous reports [6,21]. There were 16 iron atoms in each layer representing a (4×4) unit cell with a vacuum region of 25 Å. During geometrical optimization, atoms belonging to the bottom two layers of the slab were fixed at their respective bulk positions in order to mimic the bulk substrate, while the upper two layers of atoms were allowed to relax fully. The generalized gradient approximation (GGA) functional is adopted to describe the electronic exchange and correlation, in conjunction with a double numerical basis set plus polarization (DNP) atomic orbitals, where the reliability and efficiency of this level of theory has been verified by previous investigations on the relevant systems [13,14,22]. The Brillouin-zone integrations were performed using a $6 \times 6 \times 1$ special Monkhorst-Pack *k*-point grid. The DFT semicore pseudopotentials (DSPP) [23] core treat method is implemented for relativistic effects. The tolerances of energy, gradient, and displacement convergence were 1×10^{-5} Ha, 2×10^{-3} Ha Å^{-1}, and 5×10^{-3} Å, respectively. All computations were conducted with spin polarization. A Fermi smearing of 0.001 Ha was

6 used to count the orbital occupancy, and the real space cutoff of the atomic orbital was set at 4.6 Å.

For the adsorption systems, the interaction energy, E_{ads}, for the corrosion inhibitors on the iron surface is defined as:

$$E_{ads} = E_{complex} - (E_{Fe} + E_{inh}) \quad (1)$$

where $E_{complex}$ is the total energy of the iron surface and inhibitor, E_{Fe} and E_{inh} is the total energy of the iron crystal and free inhibitor molecule, respectively. According to this definition, a negative value of E_{ads} corresponds to an exothermic and spontaneous adsorption process.

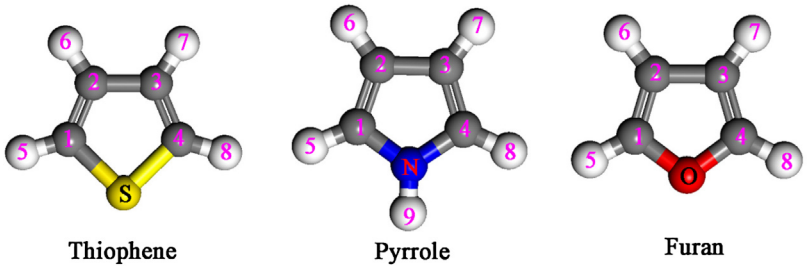

Fig. 3. Molecular structure and the atom numbering for thiophene, pyrrole, and furan.

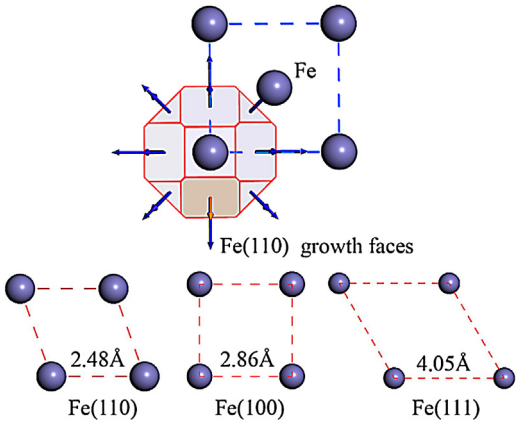

Fig. 4. Calculated structural characteristics for Fe(110), Fe(100), and Fe(111) facets.

To facilitate the presentation, the molecular structure of thiophene, pyrrole, and furan along with the numbering of atoms is presented in Fig. 3.

3. Results and discussion

3.1. Selection of adsorption surface

Firstly, it is necessary to choose an appropriate adsorption surface. Generally speaking, the surface energy, E_{surf}, can be defined as the excess energy at the surface of a material compared to the bulk [24]:

$$E_{surf} = \frac{E_{slab} - nE_{bulk}}{2S} \quad (2)$$

Herein E_{slab} and E_{bulk} are the total energies of the studied surface slab and bulk materials (*i.e.*, iron in this work), respectively. n is the number of iron formula units in the slab and S is the surface area. We use a factor "2" because each slab contains two (top and bottom) surfaces. The obtained surface energies and some morphology parameters for iron crystal are collected in Table 1. Moreover, a particularly intuitive diagram of the structural comparison for Fe(110), Fe(100), and Fe(111) facets is produced, as displayed in Fig. 4. It can be seen from Table 1 that the (110) face accounts for more than 63% of the total crystal surface area. On the other hand, the calculated surface energy values increase in the following sequence: $E_{(110)} < E_{(100)} < E_{(111)}$. It is consistent with the trend obtained from Arya et al. [25]. It should be noted that the differences of E_{surf} values between our work and Arya's data can be attributed to the functional effect and the thickness of simulated iron slab. As a whole, as for the three typical kinds of iron surfaces, Fe(111) and Fe(100) surfaces have relatively open structures, while Fe(110) is a density packed surface and has the most stabilization, so Fe(110) to was chosen for the simulation of the adsorption process.

Table 2
Adsorption energies (in eV) of three inhibitor molecules and CO adsorbed on Fe(110) as obtained with different functionals.

Functionals	Thiophene	Pyrrole	Furan	CO[b]
RPBE	−0.837	−0.660	−0.575	−1.34
PBE	−1.694	−1.378	−1.319	−1.72
PW91	−1.703	−1.359	−1.310	−1.86
RPBE-COSMO[a]	−0.788	−0.626	−0.531	

[a] Includes COSMO for implicit solvation (solvent: water, dielectric constant: 78.44).
[b] Ref. [26].

3.2. Adsorption geometries and energies

As a first step for the geometrical optimization of inhibitor/Fe(110) systems, we considered three different initial adsorption modes: (i) initial perpendicular with the O, N, and S atoms attached to the iron atoms, (ii) initial tilted mode (a certain angle about 45°) bonded to the surface, and (iii) initial parallel mode bonded to surface atoms with all the backbone atoms of the five-membered rings. Next, these configurations were all fully optimized. Our results show that both the tilted and perpendicular adsorption types are unstable, they will eventually become to the parallel configuration. Thus, in the following discussion we will only focus on the parallel adsorption mode.

The calculated adsorption energies (E_{ads}) with different functionals are given in Table 2. For comparison purposes, the adsorption energies of CO at specific site on Fe(110) [26] were also given. The negative adsorption energies indicate that the adsorptions are exothermic and stable, showing that the surface is tend to adsorb the inhibitor molecules. Looking in more detail at Table 2, notice that the PBE functional gives similar E_{ads} values compared with PW91. However, the RPBE functional shows relatively small values of E_{ads}. But they show the same trends, that is, the E_{ads} values increase in the order $E_{Furan} < E_{Pyrrole} < E_{Thiophene}$. This implies that the strength of the adsorption increases in the order Furan < Pyrrole < Thiophene. Furthermore, thiophene gives the maximum negative adsorption energy value and hence it can exhibit greater inhibition abilities relative to the Furan and Pyrrole. One other thing to note is some researchers maintain that the computed E_{ads} for small molecules on some transition metal surfaces at the RPBE functional are usually in better agreement with the experimental values than the PBE/PW91-calculated (as reviewed by Hammer and Norskov) [27,28], this is because that RPBE can more accurately describe the molecular bond energies. Then, we only give the RPBE results of the geometry optimized structures of thiophene, pyrrole, and furan adsorbed on Fe(110) (see Fig. 5), in which the conductor-like screening model (COSMO) solvation model [29] was adopted.

By careful examination of Fig. 5, it could be noticed that all the three inhibitors of interest adsorbed nearly parallel to the Fe(110) surface. Some obvious chemical bonds can be found, which originate from the donation of π electrons of five member ring as

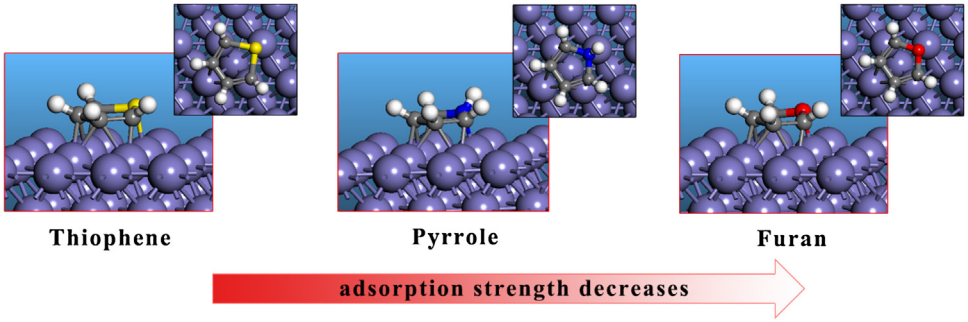

Fig. 5. Geometry optimized structures of thiophene, pyrrole, and furan adsorbed on Fe(110) (RPBE-results).

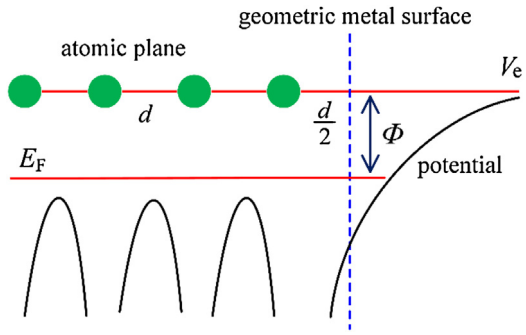

Fig. 6. Schematic energy diagram of a metal surface.

Table 3
Hirshfeld atomic charge populations of studied molecules at advantage adsorption sites on the Fe(110) surface..

Atom	Thiophene		Pyrrole		Furan	
	Free	Adsorbed	Free	Adsorbed	Free	Adsorbed
S/N/O	0.12	0.19	−0.07	−0.05	−0.06	−0.05
C1	−0.09	−0.08	−0.04	−0.02	0.00	0.00
C2	−0.07	−0.04	−0.09	−0.05	−0.08	−0.05
C3	−0.07	−0.04	−0.09	−0.05	−0.08	−0.05
C4	−0.09	−0.08	−0.04	−0.02	0.00	0.00
H5	0.05	0.05	0.05	0.05	0.06	0.06
H6	0.05	0.06	0.04	0.05	0.05	0.06
H7	0.05	0.06	0.04	0.05	0.05	0.06
H8	0.05	0.05	0.05	0.05	0.06	0.06
H9			0.15	0.14		
Total	0.00	0.17	0.00	0.15	0.00	0.09

well as the lone pair of the hetero-atoms (N, S, and O) to the metal. It is not surprising that the inhibitor molecules prefer to chemisorb strongly parallel to the surface of transition metals with open *d*-band (such as iron) with a pronounced π–*d* hybridization. This have been confirmed in our previous work [30,31] and other related findings [6,32]. The measured Fe—S, Fe—N, and Fe—O bond lengths are 2.223, 2.001, and 2.092 Å, respectively. They are comparable to the sum of the covalent radii of the two atoms involved in the bond (covalent radii are 1.05, 0.71, 0.66, 1.32 Å for S, N, O, Fe, respectively) [33]. Besides, the bond lengths predicted by theory are aslo coinciding with available experimental data obtained from multiple-scattering XAFS analyses [34] or low-energy electron diffraction (LEED) method [35,36]. This is one major reason that why they are categorized as chemisorption.

3.3. Changes of work function

The work function (Φ) is defined as the minimum energy needed by electrons at the bottom of a solid to escape externally, and can be expressed as [37]:

$$\Phi = V_e - E_F \quad (3)$$

where V_e is the vacuum level, and E_F is the Fermi level. A schematic energy diagram of a metal surface is given in Fig. 6. We define that $\Delta F = \Phi_2 - \Phi_1$, Φ_1 and Φ_2 are the work function values of clean and modified (adsorbed) metal surface, respectively. Generally, when the $\Delta\Phi > 0$, it means that the adsorbates can accept electrons from the surface. Conversely, it will donate electrons if $\Delta\Phi < 0$ [38].

In this work, the obtained Φ of clean Fe(110) surface is 4.16 eV, which is in agreement with experimental data (4.50 eV) [39]. However, the work function values of modified Fe(110) surface by thiophene, pyrrole, and furan are 3.91, 3.70, and 3.94 eV, respectively. These lower values indicate that three inhibitors are all good electron donors.

3.4. Population analysis and charge density difference

Hirshfeld Charge population analysis (see Table 3) shows that there are 0.17, 0.15, and 0.09 *e* charge transfer from the adsorbed inhibitor molecules to Fe(110) surface, suggesting that the three inhibitors of interest behave as donors and Fe(110) as acceptors. This is consistent with above work function analysis.

To better understand the adsorption mechanism of inhibitor molecules on iron surface, we calculate the charge density difference, $\Delta\rho$, which is defined as [21]

$$\Delta\rho = \rho_{mol/sur}(r) - \rho_{sur}(r) - \rho_{mol}(r) \quad (4)$$

where $\rho_{mol/sur}(r)$, $\rho_{sur}(r)$, and $\rho_{mol}(r)$ are the total density difference of the adsorption system, the clean Fe(110) surface, and the isolated inhibitor molecules, respectively.

As shown in Fig. 7, the blue areas indicate charge depletion, while the red areas represents charge accumulation. We slso present the molecular net charges below each plot, which is calculated by Hirshfeld analysis. The charge density difference visually shows the interaction between inhibitor molecules and iron surface. We can see that the area of blue regions are around the aromatic rings, while the area of red regions are around the Fe atoms. There exists an electron transfer process of the delocalized π-electrons of the aromatic rings to the Fe 3*d* orbital. Thus, these strong interactions results in large values of adsorption energies for the above three flat adsorption configurations.

3.5. Projected density of states

The information regarding the origin of chemical bonding can be obtained from the analysis of projected density of states (PDOS), as shown in Fig. 8. Gaussian broadening scheme of width was set to be 0.1 eV, and the Fermi level is set to zero.

Fig. 8 gives the PDOS of the inhibitors/Fe(110) system before and after molecule–surface interaction: the upper panels presents the

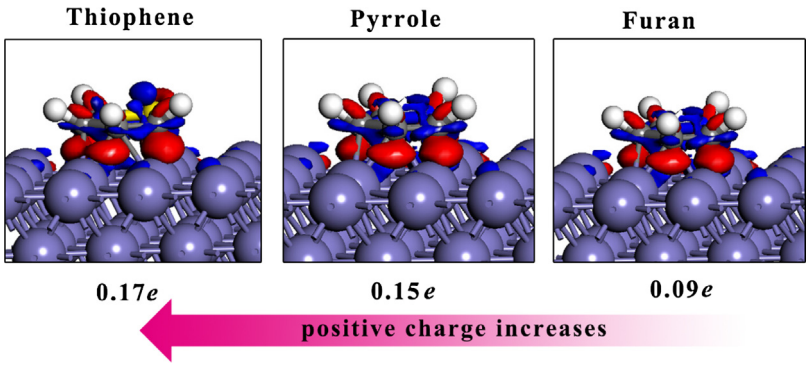

Fig. 7. Charge density difference of thiophene, pyrrole, and furan adsorbed on Fe(110) surface with the parallel adsorption configurations.

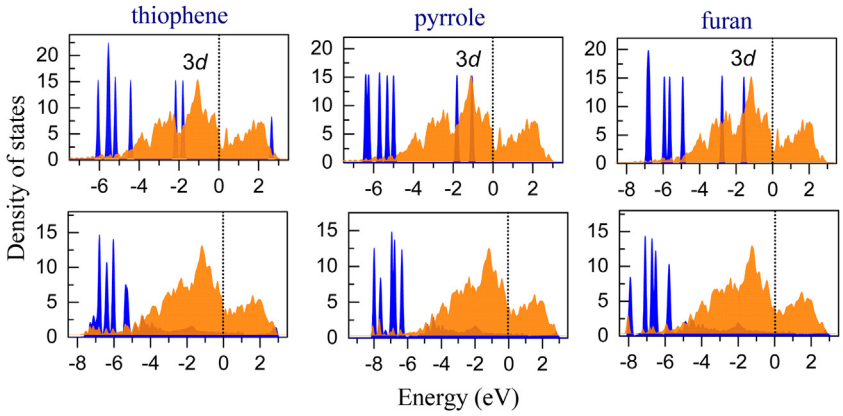

Fig. 8. Density of state of thiophene, pyrrole, and furan adsorbed on Fe(110) surface (upper panels: molecules above Fe(110); lower panels: parallel adsorption configurations in Fig. 5).

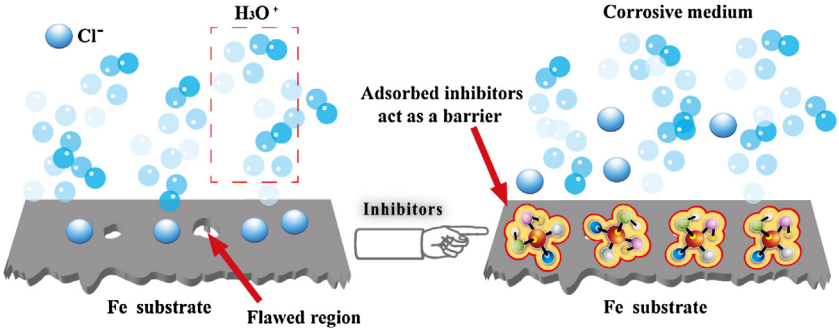

Fig. 9. Schematic diagram of the corrosion inhibition mechanism.

PDOS for the molecules located 6 Å above the Fe(110) surface, and the lower panels shows the PDOS for the molecules with optimized parallel adsorption configuration. In the figure, blue represents corrosion inhibitors and brown represents Fe atoms. From the upper panels of Fig. 8, we find that there are several molecular states lie at the position of the Fe 3*d*-band before the interactions, and these molecular orbitals will likely hybridize with metal *d*-states. When the inhibitor molecules adsorb on the Fe surfaces, the molecular peaks broadened slightly because the hybridization interaction. Consequently, the distributions of density of states for both Fe and adsorbates extend to low energy regions.

Finally, a schematic diagram of the inhibition mechanism is shown in Fig. 9. After adding a certain concentration of corrosion inhibitors to the corrosive media, the inhibitor molecules move quickly to the flawed regions to form strong coordination bonds with Fe atoms. Consequently, a protective barrier is formed to prevent corrosive particles (such as Cl^-, H_3O^+) attacking Fe surface.

4. Conclusions

In the present work, the interactions of three heterocyclic compounds and iron surface have been studied by DFT calculations. The main conclusions of this study are given below:

(1) The inhibitors containing hetero atoms are found to have high electron-donating ability and their inhibition efficiency increases in the order O < N < S.

(2) The inhibitors of interest can chemisorb onto Fe(110) with the molecular plain being nearly parallel to the surface.

(3) The energies of the π-molecular orbitals play a decisive role for the adsorption performance.

Acknowledgements

This research was sponsored by the Opening Project of Sichuan University of Science and Engineering (2016CL06), the Research Fund for the Doctoral Program of Tongren University (trxyDH1510), the Science and Technology Program of Guizhou Province (QKHJC2016-1149), the Guizhou Provincial Department of Education Fundation (QJHKYZ2016-105), and the Student's Platform for Innovation and Entrepreneurship Training Program(2016106665). We would like to thank the anonymous referees for valuable criticisms and useful suggestions that helped us to improve the quality of our present and future work.

References

[1] X.G. Li, D.W. Zhang, Z.Y. Liu, Z. Li, C.W. Du, C.F. Dong, Share corrosion data, Nature 527 (2015) 441–442.
[2] P.B. Raja, M. Ismail, S. Ghoreishiamiri, J. Mirza, M.C. Ismail, S. Kakooei, A.A. Rahim, Reviews on corrosion inhibitors: a short view, Chem. Eng. Commun. 203 (2016) 1145–1156.
[3] A. Cook, G. Frankel, A. Davenport, T. Hughes, S. Gibbon, D. Williams, H. Bluhm, V. Maurice, S. Lyth, P. Marcus, D. Shoesmith, C. Wren, J. Wharton, G. Hunt, S. Lyon, T. Majchrowski, R. Lindsay, G. Williams, B. Rico Oller, M. Todorova, S. Nixon, S.T. Cheng, J. Scully, A. Wilson, F. Renner, Y.H. Chen, C. Taylor, H. Habazaki, A. Michaelides, S. Morsch, P. Visser, L. Kyhl, A. Kokalj, Corrosion control: general discussion, Faraday Discuss. 180 (2015) 543–576.
[4] B.E.A. Rani, B.B.J. Basu, Green inhibitors for corrosion protection of metals and alloys: an overview, Int. J. Corrosion 2012 (2012) 1–15.
[5] S. Papavinasam, Corrosion inhibitors, in: R.W. Revie (Ed.), Uhlig's Corrosion Handbook, second edition, John Wiley & Sons Inc., 2000, pp. 1091–1105.
[6] N. Kovacevic, A. Kokalj, Chemistry of the interaction between azole type corrosion inhibitor molecules and metal surfaces, Mater. Chem. Phys. 137 (2012) 331–339.
[7] J. Zhang, G. Qiao, S. Hu, Y. Yan, Z. Ren, L. Yu, Theoretical evaluation of corrosion inhibition performance of imidazoline compounds with different hydrophilic groups, Corrosion Sci. 53 (2011) 147–152.
[8] A. Kokalj, Ab initio modeling of the bonding of benzotriazole corrosion inhibitor to reduced and oxidized copper surfaces, Faraday Discuss. 180 (2015) 415–438.
[9] S. Kaya, B. Tüzün, C. Kaya, I.B. Obot, Determination of corrosion inhibition effects of amino acids: quantum chemical and molecular dynamic simulation study, J. Taiwan Inst. Chem. Eng. 58 (2016) 528–535.
[10] N.O. Obi-Egbedi, I.B. Obot, M.I. El-Khaiary, Quantum chemical investigation and statistical analysis of the relationship between corrosion inhibition efficiency and molecular structure of xanthene and its derivatives on mild steel in sulphuric acid, J. Mol. Struct. 1002 (2011) 86–96.
[11] B. Cui, T. Chen, D. Wang, L.J. Wan, In situ STM evidence for the adsorption geometry of three N-heteroaromatic thiols on Au(111), Langmuir 27 (2011) 7614–7619.
[12] F. Bentiss, M. Traisnel, L. Gengembre, M. Lagrenée, A new triazole derivative as inhibitor of the acid corrosion of mild steel: electrochemical studies, weight loss determination, SEM and XPS, Appl. Surf. Sci. 152 (1999) 237–249.
[13] L. Guo, W.P. Dong, S.T. Zhang, Theoretical challenges in understanding the inhibition mechanism of copper corrosion in acid media in the presence of three triazole derivatives, RSC Adv. 4 (2014) 41956–41967.
[14] W. Wang, Z. Li, Q. Sun, A. Du, Y. Li, J. Wang, S. Bi, P. Li, Insights into the nature of the coupling interactions between uracil corrosion inhibitors and copper: a DFT and molecular dynamics study, Corrosion Sci. 61 (2012) 101–110.
[15] S. Sun, Y. Geng, L. Tian, S. Chen, Y. Yan, S. Hu, Density functional theory study of imidazole, benzimidazole and 2-mercaptobenzimidazole adsorption onto clean Cu(111) surface, Corrosionn Sci. 63 (2012) 140–147.
[16] I.B. Obot, D.D. Macdonald, Z.M. Gasem, Density functional theory (DFT) as a powerful tool for designing new organic corrosion inhibitors. Part 1: an overview, Corrosion Sci. 99 (2015) 1–30.
[17] L. Yang, Y. Dong, Crystal morphology study of N,N′-diacetylchitobiose by molecular dynamics simulation, Carbohydr. Res. 346 (2011) 2457–2462.
[18] B. Delley, From molecules to solids with the DMol3 approach, J. Chem. Phys. 113 (2000) 7756–7764.
[19] A. Juan, R. Hoffmann, Hydrogen on the Fe(110) surface and near bulk bcc Fe vacancies—a comparative bonding study, Surf. Sci. 421 (1999) 1–16.
[20] D.E. Jiang, E.A. Carter, Carbon atom adsorption on and diffusion into Fe(110) and Fe(100) from first principles, Phys. Rev. B 71 (2005).
[21] M. Ozcan, D. Toffoli, H. Ustunel, I. Dehri, Insights into surface-adsorbate interactions in corrosion inhibition processes at the molecular level, Corrosion Sci. 80 (2014) 482–486.
[22] F. Chiter, C. Lacaze-Dufaure, H. Tang, N. Pebere, DFT studies of the bonding mechanism of 8-hydroxyquinoline and derivatives on the (111) aluminum surface, Phys. Chem. Chem. Phys. 17 (2015) 22243–22258.
[23] B. Delley, Hardness conserving semilocal pseudopotentials, Phys. Rev. B 66 (2002) 155125.
[24] N.D. Lang, W. Kohn, Theory of metal surfaces-charge density and surface energy, Phys. Rev. B 1 (1970) 4555.
[25] A. Arya, E.A. Carter, Structure, bonding, and adhesion at the TiC(100)/Fe(110) interface from first principles, J. Chem. Phys. 118 (2003) 8982–8996.
[26] D.E. Jiang, E.A. Carter, Adsorption and dissociation of CO on Fe(110) from first principles, Surf. Sci. 570 (2004) 167–177.
[27] B. Hammer, J.K. Norskov, Theoretical surface science and catalysis: calculations and concepts, Adv. Catal. 45 (2000) 71–129.
[28] B. Hammer, L.B. Hansen, J.K. Norskov, Improved adsorption energetics within density-functional theory using revised Perdew-Burke-Ernzerhof functionals, Phys. Rev. B 59 (1999) 7413–7421.
[29] T. Todorova, B. Delley, Wetting of paracetamol surfaces studied by DMol3-COSMO calculations, Mol. Simul. 34 (2008) 1013–1017.
[30] L. Guo, S. Zhu, W. Li, S. Zhang, Electrochemical and quantum chemical assessment of 2-aminothiazole as inhibitor for carton steel in sulfuric acid solution, Asian J. Chem. 27 (2015) 2917–2923.
[31] R.X. Chen, L. Guo, S.Y. Xu, Experimental and theoretical investigation of 1-hydroxybenzotriazole as a corrosion inhibitor for mild steel in sulfuric acid medium, Int. J. Electrochem. Sci. 9 (2014) 6880–6895.
[32] J.O. Mendes, E.C. da Silva, A.B. Rocha, On the nature of inhibition performance of imidazole on iron surface, Corrosion Sci. 57 (2012) 254–259.
[33] P. Pyykko, M. Atsumi, Molecular single-bond covalent radii for elements 1–118, Chem. Eur. J. 15 (2009) 186–197.
[34] A.M. Rich, P.J. Ellis, L. Tennant, P.E. Wright, R.S. Armstrong, P.A. Lay, Determination of Fe-ligand bond lengths and the FeNO bond angles in soybean ferrous and ferric nitrosylleghemoglobin a using multiple-scattering XAFS analyses, Biochemistry 38 (1999) 16491–16499.
[35] M.A. Vanhove, G.A. Somorjai, Adsorption and adsorbate-induced restructuring: a LEED perspective, Surf. Sci. 299 (1994) 487–501.
[36] K. Yoshida, G.A. Somorjai, The chemisorption of CO, CO2 C2H2, C2H4, H2 and NH3 on the clean Fe(110) and (111) crystal surfaces, Surf. Sci. 75 (1978) 46–60.
[37] N. Lang, W. Kohn, Theory of metal surfaces: work function, Phys. Rev. B 3 (1971) 1215–1223.
[38] N. Kovačević, A. Kokalj, The relation between adsorption bonding and corrosion inhibition of azole molecules on copper, Corrosion Sci. 73 (2013) 7–17.
[39] H.B. Michaelson, Work function of elements and its periodicity, J. Appl. Phys. 48 (1977) 4729–4733.